Available online at www.sciencedirect.com
SCIENCE DIRECT
Free Radical Biology & Medicine 41 (2006) 657–667
www.elsevier.com/locate/freeradbiomed

Original Contribution

Properties of the radical intermediate obtained on oxidation of 2′,7′-dichlorodihydrofluorescein, a probe for oxidative stress

Marta Wrona *, Peter Wardman

Gray Cancer Institute, Mount Vernon Hospital, Northwood, Middlesex HA6 2JR, UK

Received 3 April 2006; revised 5 May 2006; accepted 5 May 2006
Available online 10 May 2006

Abstract

Reduced "leuco" dyes such as dichlorodihydrofluorescein ($DCFH_2$) are widely used as profluorescent probes for oxidative stress, although they require a catalyst to be oxidized by hydrogen peroxide and react indiscriminately with oxidizing radicals and the fluorescent product (DCF) is a potential photosensitizer of superoxide generation. In this study, key properties of the radical intermediate in oxidation ("semiquinone," $DCFH^{\bullet}$/$DCF^{\bullet-}$) were measured, to help understand the reactions that can occur in biological systems. The intermediate was generated by oxidizing $DCFH_2$ or reducing DCF by radiolytically generated radicals and monitoring the reactions using kinetic spectrophotometry. The semiquinone showed pH-sensitive absorption spectral changes, decay kinetics (both in the absence and in the presence of oxygen), and reduction potential, all corresponding to prototropic dissociations with pK_a's of ~7.1 and 9.0. $DCFH_2$ has pK_a's in a similar region (8–9) and hence pH variations are potentially important in the use of this probe. The rate constant for reaction of the semiquinone with oxygen at pH 7.4 is 5.3×10^8 M^{-1} s^{-1}: this reaction, rather than disproportionation of $DCFH^{\bullet}$/$DCF^{\bullet-}$, generates DCF in biological systems, concomitantly forming superoxide and hence H_2O_2 to cycle the catalyst. The midpoint reduction potential of the couple $DCF,H^+/DCFH^{\bullet}$ is approximately −0.75 V vs. NHE at pH 7.4; DCF is unlikely to be reduced rapidly by common flavoprotein reductases.

Keywords: Dichlorodihydrofluorescein; Fluorescent probes; Reduction potential; pK_a; Pulse radiolysis

2′,7′-Dichlorodihydrofluorescin ($DCFH_2$; Fig. 1) is widely used to measure oxidative stress in cells. Cells can be loaded with $DCFH_2$ by incubating them with the diacetate, which diffuses across the cell membrane and is hydrolyzed by intracellular esterases to liberate $DCFH_2$. Upon reaction with oxidizing species, nonfluorescent $DCFH_2$ is transformed into the highly fluorescent two-electron oxidation product, 2′,7′-dichlorofluorescein (DCF; Fig. 1). Oxidation of $DCFH_2$ and related profluorophores can occur by reaction with hydrogen peroxide *provided a catalyst is present,* such as a heme, a peroxidase, or cytochrome *c* [1–8]. DCF formation may also result from other reactive oxygen or nitrogen species [9–12], and $DCFH_2$ oxidation can actually stimulate superoxide formation [13,14]. Our previous work showed that $DCFH_2$ was oxidized to DCF rapidly and noncatalytically by nitrogen dioxide and carbonate radicals, and the fluorescent product (DCF) itself reacted with $NO_2^{\bullet}$, $CO_3^{\bullet-}$, and $^{\bullet}OH$ [12]. $DCFH_2$ can also be oxidized by pyocyanin and other oxidants [15].

Not surprisingly, then, several previous papers have stressed that the quantitation of reactive oxygen species in biological systems by oxidation of $DCFH_2$ to DCF should be approached with caution [5–9,13,14,16,17]. Thus it was demonstrated that the photoreduction of DCF in the presence of reducing agents results in formation of the DCF semiquinone free radical ($DCFH^{\bullet}$/$DCF^{\bullet-}$; Fig. 1), which under aerobic conditions is oxidized to DCF, concomitantly forming superoxide radical [13]. Reaction of $DCFH_2$ with horseradish peroxidase compound I or II generates the DCF semiquinone radical and hence superoxide [5]. DCF also reacts with horseradish peroxidase compound I or II, forming a phenoxyl free radical, structurally

Abbreviations: AQS^-, 9,10-anthraquinone-2-sulfonate; DCF, 2′,7′-dichlorofluorescein; $DCFH_2$, 2′,7′-dichlorodihydrofluorescein; MV^{2+}, methyl viologen dication (1,1′-dimethyl-4,4′-bipyridinium); NAD^+, nicotinamide adenine dinucleotide; TQ^{2+}, tetraquat (6,7,8,9-tetrahydrodipyrido[1,2-a:2′,1′-c][1,4]diazocinediium).

* Corresponding author. Fax: +1 923 835210.
E-mail address: wrona@gci.ac.uk (M. Wrona).

0891-5849/$ - see front matter © 2006 Elsevier Inc. All rights reserved.
doi:10.1016/j.freeradbiomed.2006.05.006

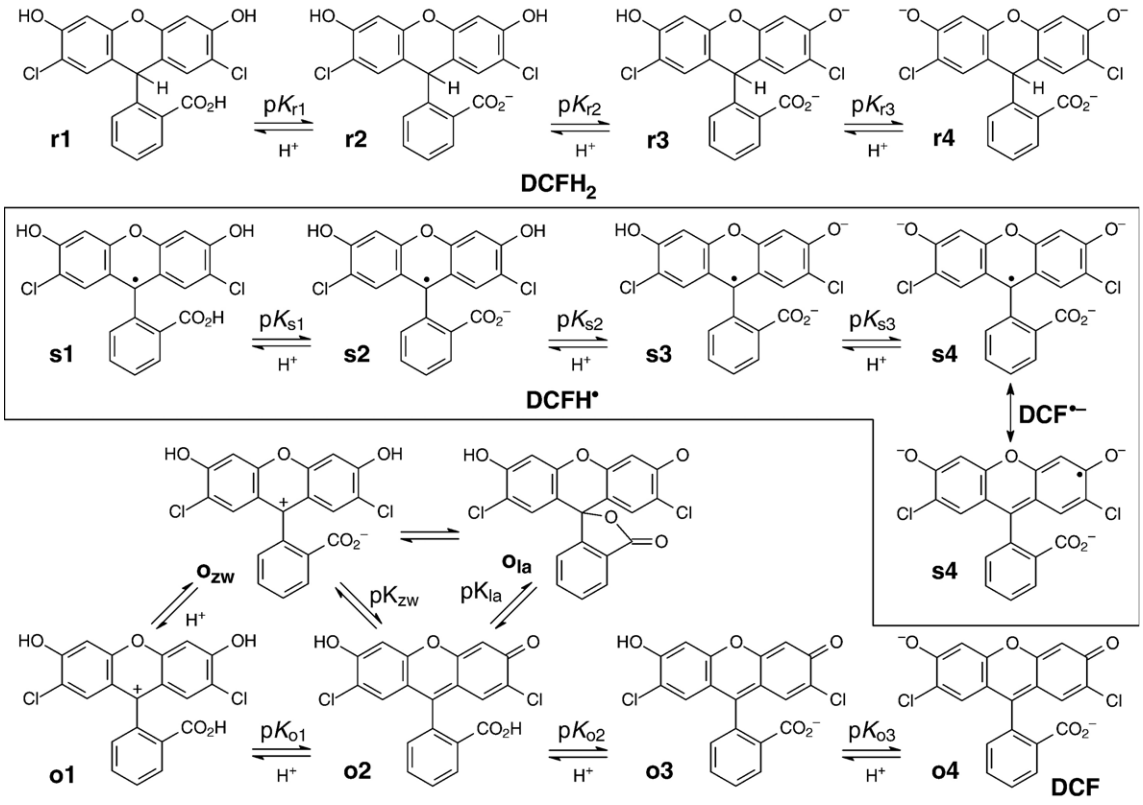

Fig. 1. Structures and prototropic dissociation equilibria of $DCFH_2$ (r1–4), $DCFH^{\bullet}/DCF^{\bullet-}$ (s1–s4), and DCF (o1–o4). One of the resonance forms of $DCF^{\bullet-}$ (s4′) and zwitterionic (o_{zw}) and lactone (o_{la}) structures of DCF are also shown.

and chemically distinct from the DCF semiquinone [16]. Reducing agents (e.g., GSH or NADH) restore the phenoxyl radical to DCF, with concomitant formation of $GS^{\bullet}$ or $NAD^{\bullet}$, respectively, which also then generate superoxide radicals. Such reducing agents will compete for the radical oxidants in noncatalytic oxidation of $DCFH_2$ [12].

To help understand these complex processes, and assess the importance of competing or complicating reactions in the use of $DCFH_2$ and similar probes, we have now measured the kinetics of the key reaction of the semiquinone radical ($DCFH^{\bullet}/DCF^{\bullet-}$) with oxygen, the kinetics of the competing radical disproportionation reaction, and the reduction potential of the oxidized probe. The latter parameter is a useful guide as to the potential reducibility of the oxidized probe by intracellular flavoprotein reductases, which commonly reflects the reduction potential of the quinone/semiquinone couple [18]. All these properties vary with pH and we have partially characterized the complex, underlying prototropic equilibria (Fig. 1). Radicals were generated by pulse radiolysis, and their reactions were monitored by fast kinetic spectrophotometry.

Materials and methods

Chemicals

All chemicals were of the highest grade available: $DCFH_2$ diacetate, DCF, sodium azide, nicotinamide adenine dinucleotide, 9,10-anthraquinone-2-sulfonate (sodium salt), methyl viologen, sodium formate, potassium thiocyanate, potassium ferricyanide, potassium chloride, acetone, 2-propanol, and buffers were from Sigma Aldrich (Poole, UK). Tetraquat dibromide salt was kindly provided by Dr. M.A. Naylor, Gray Cancer Institute. O_2 and N_2O were from British Oxygen Co. (Poole, UK). $DCFH_2$ was prepared by adding 2 mg of the diacetate to 8 ml of 10 mM NaOH, sonicating for 2 min, and allowing it to stand for 15 min in a light-protected vial [9]. The hydrolysate was brought to the required pH with phosphate buffer (5–10 mM). Solutions were stored in the dark and used immediately for experiments.

Pulse radiolysis

Experiments were performed as previously described [19]. Electron pulses of 6 MeV energy and 0.2 μs duration delivered pulses of 2–6.5 Gy, as determined by thiocyanate dosimetry [20]. An optical path cell of 2 cm was employed; all experiments were carried out at room temperature (about 22°C).

Generation of the semiquinone radical $DCFH^{\bullet}/DCF^{\bullet-}$

Radicals (typically ~1.5 μM) were produced by pulse radiolysis of aqueous solutions containing 0.1 M sodium azide or 0.1 M sodium formate and saturated with 25 mM nitrous oxide (N_2O). Radiolysis generates hydrated electrons (e^-_{aq}) and $^{\bullet}OH$ and $H^{\bullet}$ radicals in the ratio ~1:1:0.025, respectively. N_2O reacts

with e_{aq}^- to form $^\bullet OH$, which oxidizes N_3^- or HCO_2^-. The kinetics are such that ~90% of the radicals are converted to azide radicals ($N_3^\bullet$) (Eq. (1)) or formate radicals ($CO_2^{\bullet-}$) (Eq. (2)) within ~0.1 μs of the end of the pulse [21]:

$$^\bullet OH + N_3^- + H^+ \rightarrow H_2O + N_3^{\bullet-}, \quad (1)$$

$$^\bullet OH + CO_2^- + H^+ \rightarrow H_2O + CO_2^{\bullet-}. \quad (2)$$

The semiquinone radical $DCFH^\bullet/DCF^{\bullet-}$ was generated either by oxidizing $DCFH_2$ with $N_3^\bullet$ (Eq. (3)) or by reducing DCF with $CO_2^{\bullet-}$ (Eq. (4)):

$$DCFH_2 + N_3^\bullet \rightarrow DCFH^\bullet + N_3^- + H^+, \quad (3)$$

$$DCF + CO_2^{\bullet-} + H^+ \rightarrow DCFH^\bullet + CO_2. \quad (4)$$

Values of yield $G(N_3^\bullet) = 0.73$ and $G(CO_2^{\bullet-}) = 0.74$ μM Gy^{-1} were assumed, corresponding to yields at 0.1 M scavenger in N_2O-saturated water.

To analyze the kinetics of the interaction of $DCFH^\bullet/DCF^{\bullet-}$ with oxygen, samples were bubbled with mixtures of O_2 and N_2O using calibrated flowmeters (Cole-Palmer, London, UK) and oxygen was analyzed using a Model 571 paramagnetic transducer (Servomex, Crowborough, East Sussex, UK).

Redox properties of DCF

The midpoint one-electron reduction potentials of DCF at various pH_i were measured by establishing equilibria with redox indicators Ind (Eq. (5)) and measuring the equilibrium constant K_5 in microseconds, before radicals could decay [22]:

$$DCF^{\bullet-} + Ind \rightleftarrows DCF + Ind^{\bullet-}. \quad (5)$$

The couple can be represented by $E_{mi}(DCF,H^+/DCFH^\bullet)$ or at higher pH (see below) as $E_{mi}(DCF/DCF^{\bullet-})$; for convenience here we use $DCFH^\bullet$ or $DCF^{\bullet-}$ interchangeably, recognizing that at most pH values studied there is a mixture of at least two forms. The radicals $DCF^{\bullet-}$ and $Ind^{\bullet-}$ were generated by pulse radiolysis of N_2O-saturated aqueous solutions containing 2-propanol (1 M), acetone (1 M), and buffer (10 mM; acetate buffer for pH 3.7–5.6, phosphate for pH 5.8–8.0, phosphate + NaOH for pH >8). Acetone scavenges e_{aq}^-, and 2-propanol $^\bullet OH$ and $H^\bullet$ radicals to form in each case the 2-propanol radical, which reduces DCF or Ind:

$$(CH_3)_2C^\bullet OH + DCF \rightarrow (CH_3)_2CO + H^+ + DCF^{\bullet-}, \quad (6)$$

$$(CH_3)_2C^\bullet OH + Ind \rightarrow (CH_3)_2CO + H^+ + Ind^{\bullet-}. \quad (7)$$

Initially the concentrations of the radicals $DCF^{\bullet-}$ and $Ind^{\bullet-}$ reflect kinetic competition via Eqs. (6) and (7), followed rapidly by a readjustment according to Reaction 5; K_5 was measured by either the equilibrium concentrations of the radicals from the absorbance in a few tens of microseconds, and fitting the values to the appropriate function [23] using nonlinear least-squares (Origin software, Microcal, Northampton, MA), or by analysis of the kinetics of approach to equilibrium [22].

Cyclic voltammetry

Voltammograms were recorded with a computer-controlled potentiostat (Autolab PGSTAT 20 with GPES software; Windsor Scientific, Slough, UK). The three-electrode system consisted of the working disk (3 mm), glassy carbon electrode, reference saturated calomel electrode, and a platinum wire auxiliary electrode. Values were corrected to the normal hydrogen electrode (NHE). Before every scan, the working electrode was polished with alumina slurry (0.05 μm) and rinsed with water. Solutions contained 0.1 M KCl (supporting electrolyte), 0.2 mM DCF, 1 M acetone, and 1 M 2-propanol buffered with 10 mM phosphate and were bubbled with nitrogen. Experiments were at room temperature (~22°C) with a sweep rate 0.1 V/s.

Spectrophotometric measurements of prototropic equilibria in $DCFH_2$

Absorbance spectra were recorded with a Hewlett–Packard spectrophotometer (Model 8452A) using a 1-cm cuvette. $DCFH_2$ (25 μM) in 2.5 mM phosphate buffer was brought to the required pH with $HClO_4$ (60%) or NaOH (2 M), and the spectrum was recorded. Fresh samples were used for each pH to avoid photolytic degradation by the spectrophotometer source. Values of absorbance at selected wavelengths and pH were fitted to the appropriate function [24] using nonlinear least-squares to extract estimates of pK_a.

Results

Spectral and prototropic properties of $DCFH^\bullet$ (semiquinone radical)

Oxidation of $DCFH_2$ by $N_3^\bullet$ radicals resulted initially in an absorption at 350–400 nm ($DCFH^\bullet$), which decayed over ~10 ms to yield the absorption at 500 nm characteristic of DCF (Fig. 2). Absorption spectra obtained at pH 6.4 and 7.9 have different maxima (Fig. 2). The initial absorption was at 370 nm at pH 6.4, shifting to ~400 nm at pH 7.9. The formation of the radical intermediate observed at 390 nm was exponential with first-order rate constants proportional to $DCFH_2$ concentration (seven solutions, 0–95 μM), analysis providing $k_3 = (2.05 \pm 0.06) \times 10^9$ M^{-1} s^{-1} at pH 7.4. The same pH-dependent absorption spectra were obtained upon reduction of DCF by $CO_2^{\bullet-}$ (see Fig. 3, below), analysis of the kinetics of the buildup of the absorbance at 390 nm (six DCF concentrations, 0–80 μM) yielding $k_4 = (1.2 \pm 0.1) \times 10^8$ M^{-1} s^{-1} at pH 7.4.

The influence of pH on the absorptions of the radical intermediates at 370 and 405 nm was measured, generating the radical either by oxidation of $DCFH_2$ or by reduction of

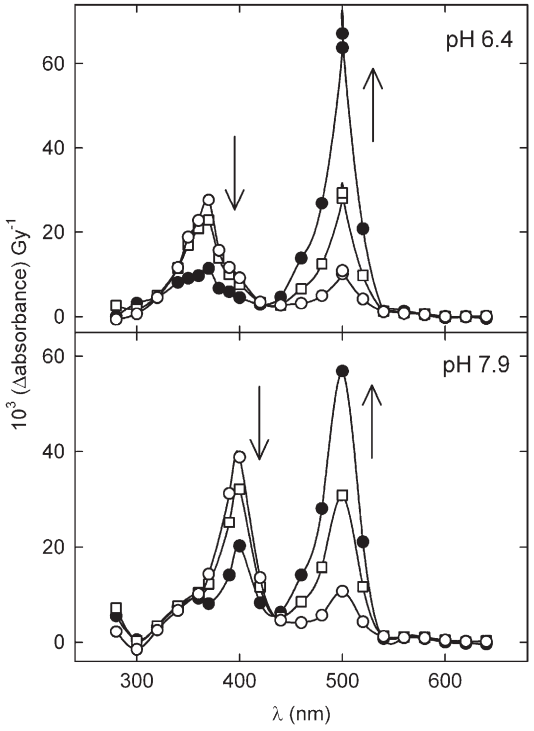

Fig. 2. Absorption spectra obtained after pulse radiolysis (~2.5 Gy) of N_2O-saturated solution of $DCFH_2$ (59 μM), NaN_3 (0.1 M), and phosphate buffer (10 mM) at pH 6.4 and 7.9 recorded 0.1 ms (○), 1 ms (□), and 8 ms (●) after the pulse.

DCF as described above. The absorption of $DCFH^{\bullet}/DCF^{\bullet-}$ at 370 nm decreased sigmoidally with increasing pH, with a concomitant increased absorbance at 405 nm (Fig. 3). Absorbance data at both wavelengths were initially fitted to the appropriate function for a single dissociation [24] to yield estimates of an apparent pK_a of 7.70 ± 0.09 (radical obtained via oxidation of $DCFH_2$) or 7.67 ± 0.07 (via reduction of DCF) at ionic strength ~0.12. That the radical(s) obtained by either route are identical was confirmed by the qualitatively similar spectral changes, the similar absolute extinction coefficients (Fig. 3), the identical apparent pK_a values, and the similar reactivities of the radical toward oxygen (see below). (Correction for the ground state absorbance of DCF but not $DCFH_2$ was necessary as pulse radiolysis measures the difference in extinction coefficients between radical and ground state.)

However, the radical "$DCFH^{\bullet}$" has several prototropic and resonance forms (Fig. 1): we expect at sufficiently high pH a trianion radical to be formed with two ionized and indistinguishable ring oxygen substituents in the xanthene moiety along with ionization of the carboxylate function. This is represented as s4 in Fig. 1, in which, following Clark [25], the prototropic forms of the reductant $DCFH_2$ are shown as r1, r2, …, as protons are lost; the forms of the oxidant DCF as o1, o2, …; and the intermediate radical or semiquinone as s1, s2, …. As protons are successively added to s4, there should be *two* distinguishable pK_a's for step-wise protonation at oxygen in the xanthene moiety (pK_{s3} and pK_{s2}, Fig. 1). From statistical considerations these two pK_a's must differ by at least $\log_{10}(4)$, i.e., 0.6, but the difference is likely to be higher [24,26]; hence our data suggest approximate bounds for pK_{s2} <7.4 and pK_{s3} >8.0. We therefore reanalyzed the data in Fig. 3 assuming the changes reflected these two pK_a's, despite the lack of obvious evidence for three rather than two species with clearly different absorbing spectra. Support for this approach was provided from analysis of pH-dependent redox and kinetic properties (see below). The solid and dashed lines in Fig. 3 represent fits to two or one dissociation, respectively; the fit to two pK_a's was superior with all of the data sets, e.g., Fig. 3A, 370 nm. Analysis according to two overlapping ionizations yielded statistically distinguishable values, and from four data sets (via DCF oxidation, DCF reduction, two wavelengths) we estimate pK_{s2} = 7.3 ± 0.2 and pK_{s3} = 8.8 ± 0.5.

Disproportionation of $DCFH^{\bullet}/DCF^{\bullet-}$

The kinetics of formation of DCF after generating $DCFH^{\bullet}$ (via oxidation of $DCFH_2$ with $N_3^{\bullet}$) was also pH-dependent. Kinetic data exhibited more random error than absorbance measurements, and for simplicity the pH dependence of radical disproportionation was analyzed according to a single dissociative equilibrium. The formation of DCF can reasonably be assigned

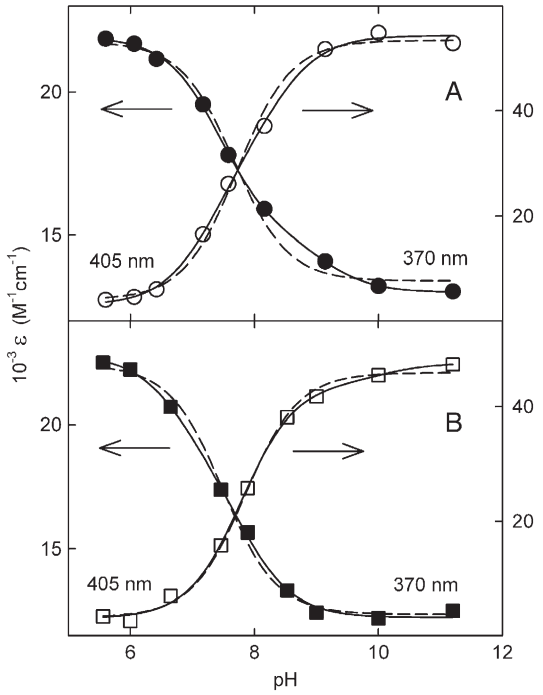

Fig. 3. Influence of pH on absorbance of radical species produced by pulse radiolysis (~2.6 Gy) of N_2O-saturated solutions of (A) $DCFH_2$ (59 μM), NaN_3 (0.1 M), phosphate buffer (10 mM), or (B) DCF (50 μM), $NaHCO_2$ (0.1 M), phosphate buffer (10 mM). Observations were made at 370 nm (●, ■; left axes) or at 405 nm (○, □; right axes). The solid lines are the fits including two dissociations (pK_a) and the dashed lines the fits to a single pK_a.

to disproportionation such as Reactions (8a)–(8c),

$$2DCFH^{\bullet} \rightarrow DCFH_2 + DCF, \quad (8a)$$

$$DCFH^{\bullet} + DCF^{\bullet -}(+H^+) \rightarrow DCFH_2 + DCF, \quad (8b)$$

$$2DCF^{\bullet -}(+2H^+) \rightarrow DCFH_2 + DCF, \quad (8c)$$

where $DCFH^{\bullet}$ represents the multiple forms s2 and s3 (Fig. 1) and $DCF^{\bullet -}$ is s4, s4′, etc.

The overall second-order rate constant $2k_{8obs}$ defined by $-d[R]/dt = 2k_{8obs}[R]^2$, where [R] is the sum of all prototropic forms of the radical, derived from observations at 500 nm (Fig. 4), was fitted to the appropriate function [27] by nonlinear least-squares (Origin), with k_{8a}, k_{8b}, k_{8c}, and pK_a as adjustable parameters, yielding an apparent pK_a of 7.54 ± 0.14 at ionic strength ~0.12. This is sufficiently close to the apparent pK_a value obtained from absorbance measurements (7.70 ± 0.09, Fig. 3, above) that we conclude the pH dependence of the rate constant is ascribable to the same prototropic phenomena. Interpolation yields an effective rate constant for disproportionation ($2k_8$) at pH 7.4 of (2.8 ± 0.3) × 10^8 M^{-1} s^{-1}. Fitting the data to a function with two pK_a's, representing reaction of three species s2, s3, and s4, was not attempted as there are six cross-reactions of the species, even ignoring involvement of s1.

Reactivity toward oxygen of the radical intermediate obtained on oxidation of DCFH$_2$ or reduction of DCF

Using pulse radiolysis, we generated ~1 to 2 μM radicals (via $N_3^{\bullet}$ or $CO_2^{\bullet -}$) from solutions of $DCFH_2$ (59 μM) and NaN_3 (0.1 M) or DCF (50 μM) and $NaHCO_2$ (0.1 M), respectively, containing 10 mM phosphate buffer and saturated with mixtures of N_2O and O_2. The amplitude of the initial absorbances at 390 nm ascribed to the semiquinone radicals were decreased relative to oxygen-free solutions,

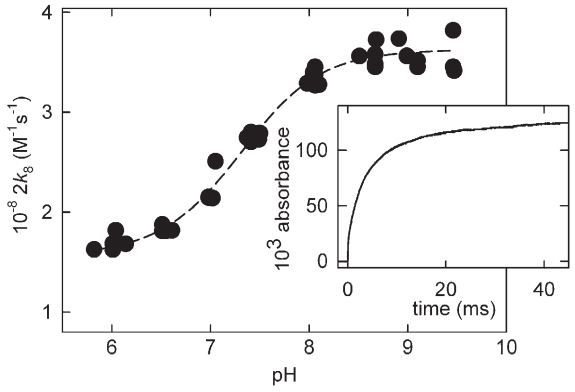

Fig. 4. Influence of pH on the second-order rate constant for the formation of DCF from $DCFH^{\bullet}/DCF^{\bullet -}$ observed at 500 nm. Radicals were generated by pulse radiolysis of N_2O-saturated solutions of $DCFH_2$ (59 μM), NaN_3 (0.1 M), and phosphate buffer (10 mM). Inset: Absorbance changes at 500 nm and pH 7.1 after a dose of ~2 Gy. Curve is the fit to an apparent single pK_a.

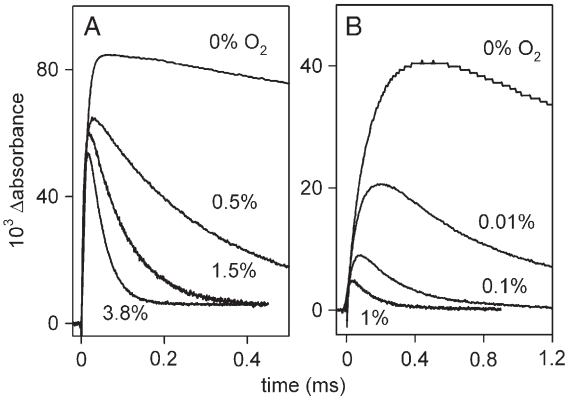

Fig. 5. Absorbance/time traces observed at 390 nm on reaction of (A) $DCFH_2$ with $N_3^{\bullet}$ and 0–3.8% oxygen (balance N_2O) or (B) DCF with $CO_2^{\bullet -}$ and 0–1% oxygen (balance N_2O) at pH 7.4, after pulse radiolysis (~3 Gy) of solutions of $DCFH_2$ (59 μM), NaN_3 (0.1 M) or DCF (50 μM), sodium formate (0.1 M), respectively, with 10 mM phosphate buffer.

either by decay occurring concomitant with radical formation or (in the case of reduction of DCF by $CO_2^{\bullet -}$) competing reaction of $CO_2^{\bullet -}$ with O_2. Analysis of the exponential decay, allowing for concomitant signal formation, was possible up to 10% O_2 v/v in the $N_3^{\bullet}/DCFH_2$ system and up to 1% O_2 in the $CO_2^{\bullet -}$/DCF system (Fig. 5). The rate constants were first order in oxygen concentration (Figs. 6A and 6B), with similar values for the second-order rate constants ascribed to reaction of the semiquinone radical with oxygen obtained producing the radical via $N_3^{\bullet}/DCFH_2$ or $CO_2^{\bullet -}$/DCF, but with the rate constant varying with pH in the range 6–9 (Fig. 6C). Again preliminary analysis corresponding to a single prototropic change yielded an apparent pK_a of 7.65 ± 0.20 but treatment according to Reaction (9) encompassing concurrent reactions of three species, s2, s3, and s4, with oxygen, with pK_{s2} = 7.3 and pK_{s3} = 8.8 from absorbance data, provided estimates of rate constants for reaction of these three species with O_2 of (3.1 ± 0.3), (7.1 ± 0.5), and (9.8 ± 0.7) × 10^8 M^{-1} s^{-1}, respectively:

$$DCF^{\bullet -}(DCFH^{\bullet}) + O_2 \rightarrow DCF + O_2^{\bullet -}(+H^+). \quad (9)$$

Interpolation indicated an effective rate constant for reaction of $DCFH^{\bullet}/DCF^{\bullet -}$ with O_2 of (5.3 ± 0.6) × 10^8 M^{-1} s^{-1} at pH 7.4.

Reduction potential of DCF characterizing reduction to the radical

The midpoint potentials of the one-electron couple E_{mi}(DCF, $H^+/DCFH^{\bullet}$) were measured by establishing electron-transfer equilibria with suitable redox indictors (Eq. (5)). Indicators (Ind) used were nicotinamide adenine dinucleotide (NAD^+), methyl viologen (MV^{2+}), tetraquat (TQ^{2+}), and 9,10-anthraquinone-2-sulfonate (AQS^-), assuming one-electron reduction potentials of −0.93, −0.450, −0.65, and −0.396 V, respectively [22,23].

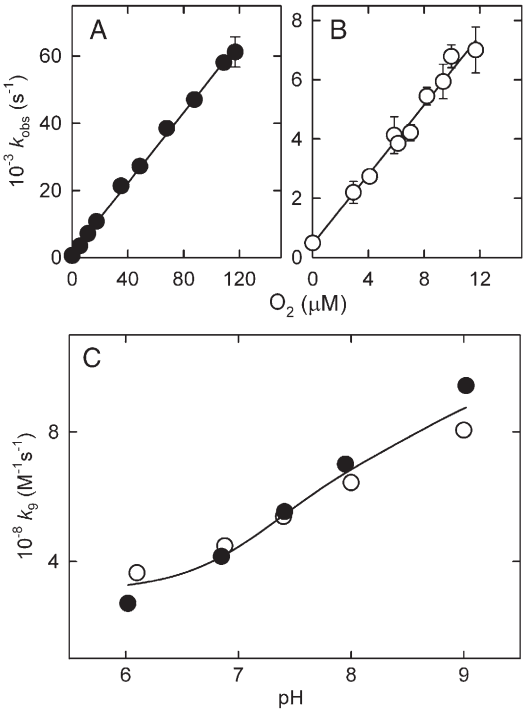

Fig. 6. Dependence on oxygen concentration of the first-order rate constant for decay of DCFH$^{\bullet}$/DCF$^{\bullet-}$ produced via (A) $DCFH_2/N_3^{\bullet}$ or (B) $DCF/CO_2^{\bullet-}$ at pH 7.4. (C) Influence of pH on the rate constant for the reaction between oxygen and radical intermediate obtained from oxidation of $DCFH_2$ (●) or reduction of DCF (○). The curve is the fit of the combined data to Reaction (9) involving three radical species linked by two prototropic dissociations.

Redox equilibria between NAD^+ and DCF were characterized for pH 7.9–10.3 using solutions containing 20 μM DCF and 0–8 mM NAD^+, monitoring $DCF^{\bullet-}$ at 390 nm. Equilibrium was established in ~200 μs, as illustrated in Fig. 7A, the data yielding a value of $K_5 = 0.0175 \pm 0.0015$ at pH 8.6 and ionic strength 0.01. Kinetic analysis of the approach to equilibrium (which usually involves greater uncertainty) was reasonably consistent with the fit to the equilibrium absorbance, with k_5 and $k_{-5} = (3.0 \pm 0.3) \times 10^6$ and $(3.0 \pm 0.4) \times 10^8\ M^{-1}\ s^{-1}$, respectively ($K_5 = 0.010 \pm 0.002$). Similar experiments were conducted using MV^{2+} (pH 3.9–5.2) or AQS^- (pH 3.4–4.5) as redox indicator, typically using 100–200 μM DCF and 10–100 μM MV^{2+} or AQS^-; data for the former indicator are shown in Fig. 7B. The typical transient again shows that Eq. (5) was established within ~200 μs, before significant decay of DCFH$^{\bullet}$ radicals via Reaction (8) at the low radical concentrations (doses) used. Illustrative values for k_5 and k^-_5 were $(1.1 \pm 0.2) \times 10^8$ and $(3.7 \pm 0.6) \times 10^7\ M^{-1}\ s^{-1}$ for Eq. (5) with Ind MV^{2+} at pH 3.9 and $(3.4 \pm 0.2) \times 10^9$ and $(4.8 \pm 0.6) \times 10^7\ M^{-1}\ s^{-1}$ for Ind AQS^- at pH 4.1.

Fig. 8 shows the pH-dependent values of the reduction potentials of the couple $E_{mi}(DCF,H^+/DCFH^{\bullet})$ derived from the measurements of K_5. Fitting the data to the theoretical dependence on pH requires values of pK_{o1}, pK_{o2}, and pK_{o3} for DCF [22,25]. We also included values of pK_{zw} and pK_{la} in the expression (0.14 and 2.0, respectively [28]) and hence for consistency values of pK_{o1}, pK_{o2}, and pK_{o3} from the same study (0.85, 3.5, and 5.19, respectively [28]). The latter are not very different from those reported earlier, uncorrected for ionic strength (0.5, 3.5, 5.0, respectively [29]). Attempted analysis varying four parameters ($E°$(DCF/DCF$^{\bullet-}$), pK_{s1}, pK_{s2}, and pK_{s3}) gave estimates of $E°(DCF/DCF^{\bullet-}) = E°(o4/s4) = -0.86 \pm 0.01$ V and pK_{s2} and $pK_{s3} = 6.95 \pm 0.13$ and 9.17 ± 0.21, respectively, but the fit did not provide a statistically significant value of pK_{s1}. The values for pK_{s2} and pK_{s3} were similar to those obtained independently from radical absorbance data (7.3 ± 0.2 and 8.8 ± 0.5), adding confidence to this treatment, and we show in Fig. 8 curves which are the fit with $E°(DCF/DCF^{\bullet-}) = -0.86$ V, pK_{s2} and pK_{s3} as 6.95 and 9.17, and $pK_{s1} = 3$, 4, or 5 to illustrate the sensitivity to the latter, uncharacterized parameter. The data points were not corrected for ionic strength, a correction which requires assumptions of net charge and therefore pK_a's and is complex at intermediate pH values; the combination of systematic errors in E_{obs} (from the redox indicator value and ionic strength effects) could add to approximately ±0.02–0.03 V. We therefore can deduce only that

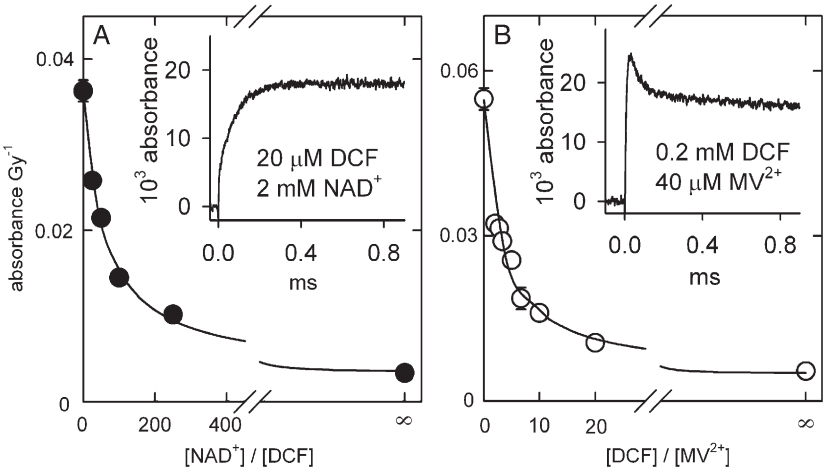

Fig. 7. Redox equilibria between DCFH$^{\bullet}$/DCF$^{\bullet-}$ and either (A) NAD^+ or (B) MV^{2+}. Radicals were generated by pulse radiolysis (~1.2 Gy) of N_2O-saturated solutions of (A) DCF (20 μM), NAD^+ (0–2 mM), 2-propanol (1 M), acetone (1 M), and phosphate buffer (10 mM), pH 8.6, and (B) DCF (0.2 mM), MV^{2+} (40 μM), 2-propanol (1 M), acetone (1 M), and acetate buffer (10 mM), pH 3.9. Insets: Transient absorbances at 390 nm.

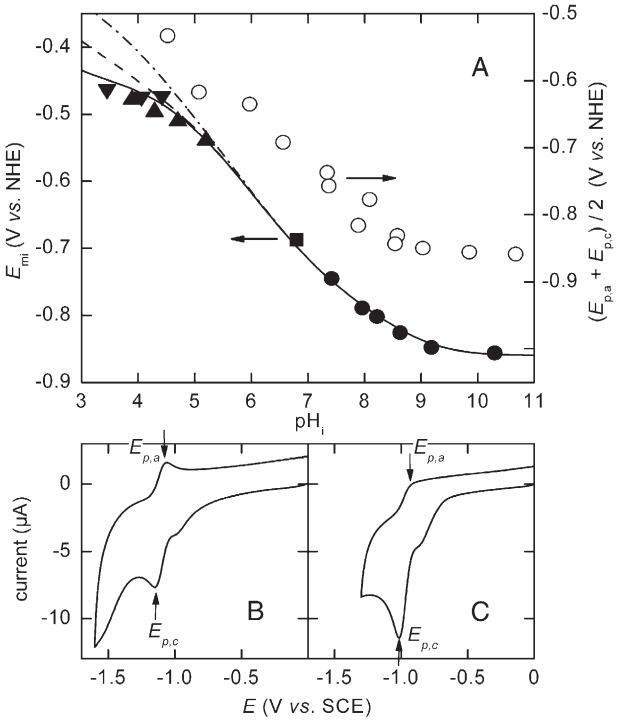

Fig. 8. (A) Variation in the reduction potential, E_{mi}(DCF,H$^+$/DCFH$^\bullet$), with pH$_i$. Reduction potentials were estimated from the equilibrium absorbances after redox equilibrium with indicators NAD$^+$ (●), TQ^{2+} (■), MV^{2+} (▲), or AQS$^-$ (▼). The curves show the fits to the theoretical dependence with the parameters given in the text, with pK_{s1} = 3 (solid line), 4 (dashed line), or 5 (dash–dot line). The estimated mean of the anodic and cathodic peak potentials from cyclic voltammetry are also shown (○), right axis (displaced vertically for clarity compared to left axis). (B, C) Cyclic voltammograms of DCF vs saturated calomel electrode at glassy carbon at pH 10.7 (B) or 7.4 (C), obtained with a sweep rate of 0.1 V/s in solutions containing DCF (0.2 mM), acetone (1 M), 2-propanol (1 M), and KCl (0.1 M, supporting electrolyte).

pK_{s1} is in the region 3–4, particularly as nothing is known about the possibility of other tautomeric forms of the radical at low pH as found with DCF.

A midpoint potential E_{mi}(DCF,H$^+$/DCFH$^\bullet$) of approximately −0.75 V was interpolated at pH$_i$ 7.4 from the data in Fig. 8.

Cyclic voltammetry of DCF

We also investigated the reduction of DCF using cyclic voltammetry. Only at high pH (e.g., ∼10.7, Fig. 8C) did the voltammograms demonstrate the form approaching that characteristic of reversibility, with increasingly irreversible behavior at lower pH. The half-wave potential was estimated from the mean of the peak anodic and cathodic waves. This was pH-dependent as shown in Fig. 8A; the value of $E_{1/2}$ = −0.86 ± 0.01 V vs. NHE at pH ∼11 was identical to the estimate of $E°$(DCF/DCF$^{\bullet-}$), i.e., $E°$(o4/s4), obtained by pulse radiolysis. The voltammograms showed evidence of a second, less well-defined redox process (the inflection at potentials more positive than $E_{p,c}$), which might be associated with further reduction of the radical. In earlier polarographic studies [30], two irreversible waves were also reported, although the second at more negative potentials than the first. However, at high pH the half-wave potential of the first wave was approximately −0.88 V vs. NHE, consistent with our data.

Varying charge on the radical DCFH$^\bullet$/DCF$^{\bullet-}$ as a function of pH

The reactivity of species usually varies with ionic strength if the reactant partners are both charged; the net charge on the radical controls the magnitude of the primary kinetic "salt effect," with a plot of $\log_{10}k_{obs}$ vs. the square root of ionic strength (or an extended function) approximating the product of charges on the reactants [27,31]. We used ionic strength effects on the kinetics of the oxidation of DCFH$^\bullet$/DCF$^{\bullet-}$ by ferricyanide ($Fe(CN)_6^{3-}$) to further understanding of the prototropic equilibria in the radical. The probe radicals were generated by pulse radiolysis of solutions containing DCF and 2-propanol/acetone (Eq. (6)), adding KCl as an inert salt, and values of rate constants for Reaction (10) were estimated as a function of ionic strength I and pH:

$$DCF^{\bullet-}(DCFH^\bullet) + Fe(CN)_6^{3-} \rightarrow DCF(+H^+) + Fe(CN)_6^{4-}. \quad (10)$$

Estimates of $\log_{10}(k_{10obs})$ (as pseudo-first-order rate constants) obtained at a single concentration of $Fe(CN)_6^{3-}$ were plotted against a function of ionic strength I using an extended Debye–Hückel–Davies expression [31] (Fig. 9A). The overall rate constants k_{10obs} for Reaction (10) extrapolated to I = 0 and the slopes of the plots of $\log_{10}(k_{10obs})$ vs. the ionic strength function are shown as a function of pH (Fig. 9B). At pH ∼4, ionic strength had no measurable effect on the kinetics of Reaction (10), suggesting that the reaction was dominated by the radical s1, which has 0 net charge. As the pH increased, the rate constant for Reaction (10) at zero ionic strength decreased steadily (by a factor of ∼50 between pH ∼4 and 11), reflecting the expected increasing Coulombic repulsion of the reactants as the charge on DCFH$^\bullet$/DCF$^{\bullet-}$ became increasingly negative, and consistent with multiple prototropic species; the slope of the plots of $\log_{10}(k_{10obs})$ vs. the ionic strength function paralleled changes in rate with pH (Fig. 9B).

The curve fitted to the I = 0 data in Fig. 9B was obtained by using the appropriate function [24,27], fixing pK_{s2} = 7.1 and pK_{s3} = 9.0 (the means of estimates from the dependencies upon pH of radical absorbance and midpoint reduction potential, see above), with pK_{s1} as an adjustable parameter along with rate constants for reaction of $Fe(CN)_6^{3-}$ with the four prototropic forms of DCFH$^\bullet$/DCF$^{\bullet-}$. Estimates of pK_{s1} = 4.9 ± 0.2 and k_{10} (at I = 0) of (1.1 ± 0.1) × 10^9, (3.6 ± 0.4) × 10^8, (9 ± 1) × 10^7, and (2.7 ± 0.3) × 10^7 M^{-1} s^{-1} for reaction of s1, s2, s3, and s4, respectively, were derived. (Note that the rate data refer to analysis at a single concentration of $Fe(CN)_6^{3-}$, although systematic errors arising from parallel radical disproportionation are thought to be small.) To illustrate the sensitivity of the fit upon the poorly characterized variable pK_{s1} (see above), the dashed lined in Fig. 9B represents the fit with pK_{s1} fixed at 4.0 and pK_{s2} and pK_{s3} as above; whereas the value of k_{11}(s1) increased from

(1.1 ± 0.1) to (1.7 ± 0.2) × 10^9 M^{-1} s^{-1} as pK_{s1} was decreased from 4.9 to 4.0; k_{11} for s2, s3, and s4 were essentially unchanged at (4.4 ± 0.4) × 10^8, (8.0 ± 0.2) × 10^7, and (2.7 ± 0.4) × 10^7 M^{-1} s^{-1}, respectively.

The pH dependence of the slope of the plots of $\log_{10}(k_{10obs})$ vs. the ionic strength function is not amenable to quantitative analysis as a function of pH because the function is both complex and multivariate. However, bearing in mind that the higher rate constants for the lesser charged reactants weight significantly the dependence to skew the slope value to lower values than might superficially be expected at a given pH, and that kinetic salt effects plots often somewhat underestimate the theoretical slope at the ionic strengths used [27], we consider that the "slope" data are consistent with pK_{s2} and pK_{s3} ~7.1 and 9.0, respectively.

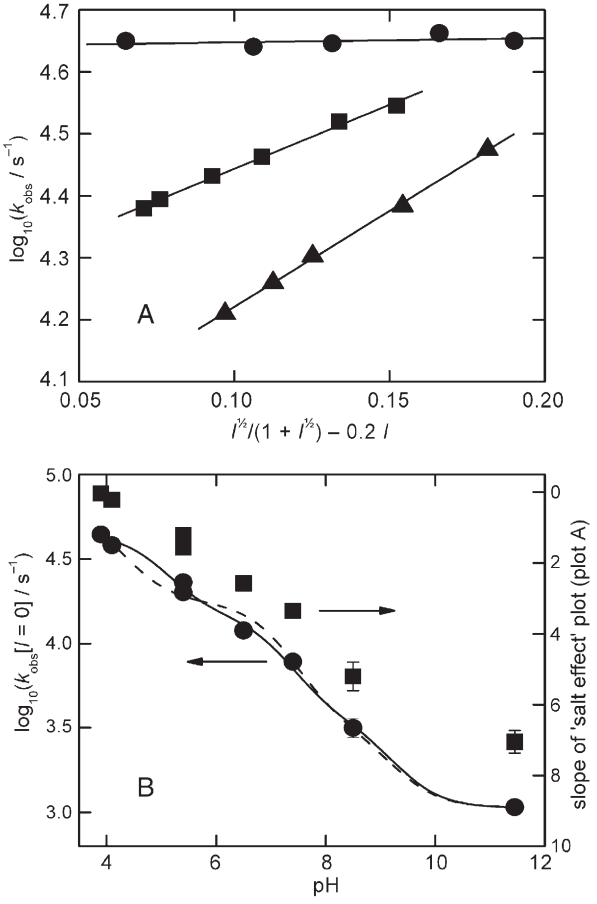

Fig. 9. (A) Effects of ionic strength on the reaction of DCFH•/DCF•− with $Fe(CN)_6^{3-}$ (40 μM), at pH 3.9 (●), pH 5.4 (■), or pH 7.4 (▲). (B) Variation with pH of the pseudo-first-order rate constant extrapolated to zero ionic strength (●). The curve (solid line) is the fitted relationship to reaction involving four radicals linked via three prototropic equilibria with pK_{s2} = 7.1 and pK_{s3} = 9.0, yielding pK_{s1} = 4.9; the dashed line illustrates the effect of setting pK_{s1} to 4.0. The slopes of the plots of log10 k vs the ionic strength function (examples in A) are shown to vary with pH in plot B (■, right axis). Data from pulse radiolysis (~3 Gy) of N_2O-saturated solutions of DCF (0.2 mM), $K_3Fe(CN)_6$ (40 μM), 2-propanol (1 M), acetone (1 M), and buffer (10 mM, acetate or phosphate buffer), with KCl (0–40 mM), are shown. Decay of DCFH•/DCF•− was observed at 370 or 390 nm.

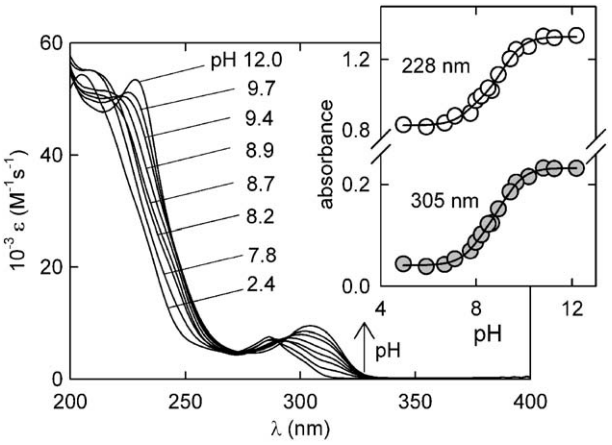

Fig. 10. Absorption spectra of $DCFH_2$ (25 μM) in solutions of phosphate buffer (10 mM) at pH 2.4–12.0. Inset: The dependence of absorbance on pH at 228 or 305 nm.

Prototropic properties of $DCFH_2$

The absorption spectra of aqueous solutions of $DCFH_2$ as a function of pH in the range 2.4–12 were recorded showing a blue shift with increasing acidity (Fig. 10). The values of absorbance at 228, 286, 305, and 315 nm between pH ~5–12 were fitted to the appropriate functions [24]. Again, a single dissociation would suggest an apparent pK_a = 8.68 ± 0.05, but pK_{r2} and pK_{r3} must differ by at least 0.6 and analysis suggested pK_{r2} = 7.9 ± 0.1 and pK_{r3} = 9.20 ± 0.02 at ionic strength ~0.01. Measurements at 228 nm and pH <5 revealed changes which might correspond to pK_{o1} in the region 3–4, but analysis was not attempted.

Discussion

The primary goals of this study were to characterize three key parameters involving the dichlorofluorescein "semiquinone" radical around physiological pH: the rate constant for the possible competing reactions of radical/radical disproportionation to form DCF and that for the reaction of the radical with oxygen and the midpoint reduction potential of the DCF,H^+/DCFH• couple. The fluorescein semiquinone radical was reported to dissociate with an apparent pK_a = 9.5 [32], and the electron-withdrawing chlorine substituents in DCFH• were expected to result in a lower value for corresponding dissociation(s) in DCFH•, perhaps near 7. It was therefore also desirable to measure the variation in these properties with pH, focusing for the present purposes on values around physiological. In the event the properties varied considerably in the physiological pH range, including the pK_a's of the parent probe $DCFH_2$, and we decided to attempt a rigorous fit of the data to the appropriate functions to derive estimates of some of the equilibrium constants that defined the pH dependence of these properties. Taken alone, extracting two pK_a values from data such as those in Fig. 2 would be at best speculative, even though theory requires multiple pK_a's and pK_{s2} ≠ pK_{s3}. However, by combining kinetic and thermodynamic data it became clear that treatment of multiple pK_a's near physiological

pH values was essential for a quantitative understanding of these variations.

Oxidation of $DCFH_2$ by $N_3^{\bullet}$ ($k_3 \sim 2.1 \times 10^9$ M^{-1} s^{-1} at pH 7.4) or reduction of DCF by $CO_2^{\bullet-}$ ($k_4 \sim 1.2 \times 10^8$ M^{-1} s^{-1} at pH 7.4, ionic strength ~ 0.12) generated the same species, assigned to the semiquinone radical, absorbing at ~370 nm at pH ~6 but shifting to ~400 nm at pH >8. Flash photolysis studies of fluorescein similarly provided evidence for a radical absorbing at 355 nm in acid but 394 nm in alkali [32]; reduction of fluorescein by $CO_2^{\bullet-}$ at pH 9.2 gave a radical absorbing at 395 nm [33]. The $DCFH^{\bullet}/DCF^{\bullet-}$ radical decayed in the absence of oxygen in a few milliseconds at micromolar initial concentrations, to form the characteristic absorbance at 500 nm of DCF. The half-life of the semiquinone radical at pH 7.4 at any initial concentration [R] with respect to disproportionation may be estimated from the formula $t_{1/2} = (2k_8[R])^{-1}$ [27], with $2k_8 \sim 2.8 \times 10^8$ M^{-1} s^{-1}. In the presence of oxygen, the semiquinone radical intermediate decayed rapidly, with the rate constant $k_9 \sim 5.3 \times 10^8$ M^{-1} s^{-1} at pH 7.4. The radical half-life in solutions containing oxygen can be estimated as $t_{1/2} \sim 0.7/(k_9[O_2])$ if $[R] \ll [O_2]$ and in the absence of other reactions [27].

In biological systems, oxidation of $DCFH_2$ to DCF proceeds either by reaction of a peroxidase compound I-like intermediate (generated on reaction of a heme with hydrogen peroxide) or directly by uncatalyzed oxidation (e.g., with $NO_2^{\bullet}$, $CO_3^{\bullet-}$, $^{\bullet}OH$ [12], or thiyl radicals (M. Wrona, unpublished work)). In both scenarios the radical intermediate $DCFH^{\bullet}$ is formed as an obligate intermediate. Under most common experimental situations, oxidation of $DCFH_2$ to $DCFH^{\bullet}$ will result in DCF formation via reaction of $DCFH^{\bullet}$ with oxygen (Reaction (9), concomitantly generating superoxide radicals [13]) rather than via disproportionation (Reaction (8)). This is easily demonstrated by considering a hypothetical scenario with 40 μM O_2 (e.g., well-oxygenated tissue, but one-fifth the nominal O_2 concentration in air-equilibrated cell cultures at 37°C) and a rate of $DCFH^{\bullet}/DCF^{\bullet-}$ radical production as high as ~0.6 mM s^{-1}, 1000-fold higher than the estimated normal rate of superoxide production in mitochondria [34]. The steady-state concentration of $DCFH^{\bullet}/DCF^{\bullet-}$ at pH 7.4 (if controlled only by Reaction (9) with O_2 and disproportionation (Reaction (8)) is calculated as ~28 nM from the positive root of the quadratic formulation of the steady-state expression; reaction of $DCFH^{\bullet}/DCF^{\bullet-}$ with O_2 is thus ~2700-fold faster than disproportionation under these conditions. Our data show that the reaction of $DCFH^{\bullet}/DCF^{\bullet-}$ with O_2 to generate superoxide [13,14] is a critical reaction responsible for the chain propagation of the oxidation of $DCFH_2$ by H_2O_2, completely overwhelming disproportionation of the $DCFH^{\bullet}/DCF^{\bullet-}$ radical as a route to DCF under most likely experimental conditions. (Of course, in the hypothetical scenario above of $DCFH^{\bullet}$ production at the high rate of ~0.6 mM s^{-1}, the probe could be depleted in seconds because typical intracellular loading via the diacetate seems unlikely to exceed ~1 mM; in representative experiments with V79 hamster fibroblasts our colleague Mrs. L.K. Folkes measured intracellular concentrations of $DCFH_2$ of ~0.3 mM.) In the above scenario $DCFH^{\bullet}/DCF^{\bullet-}$ is converted to DCF by O_2 in <100 μs; this implies DCF is generated within 1 μm of the site of production of the probe radical because the diffusion coefficient D will be less than 1×10^{-9} m^2 s^{-1} and the diffusion distance $\sim(6Dt)^{1/2}$.

The absorbance of the radical (at two wavelengths), the rate of the radical disproportionation to form DCF, and the reactivity of the radical toward oxygen all varied significantly with pH around the physiological range. The variation of all three independent properties of the semiquinone radical with pH was analyzed, all yielding an apparent value for a prototropic dissociation with $pK_a \sim 7.7$. Consideration of the required inequality of pK_{s2} and pK_{s3} led us to extract estimates of 7.3 ± 0.2 and 8.8 ± 0.5, respectively. Analysis of the pH dependence of the midpoint potential of the couple $E(DCF,H^+/DCFH^{\bullet})$ strongly supported this otherwise tentative extraction, with independent estimates of pK_{s2} and $pK_{s3} = 6.95 \pm 0.13$ and 9.17 ± 0.21. The pH dependence of the rate constant at zero ionic strength for reaction between $DCFH^{\bullet}/DCF^{\bullet-}$ and $Fe(CN)_6^{3-}$ was consistent with pK_{s2} and $pK_{s3} \sim 7.1$ and 9.0, respectively, as were the changes in the effects of ionic strength on the rate constant. Quite different ESR spectra were observed generating $DCFH^{\bullet}/DCF^{\bullet-}$ at pH 7.4 and 11.5 [13], consistent with our data, although the steady-state spectra reflect multiple pH-dependent reactions and the pH dependence may not parallel pK_a's exactly. However, our data could not provide reliable estimates of pK_{s1}, which we suggest should be around 4 (cf. benzoic acid, $pK_a \sim 4.2$). Somewhat higher values of K_{la} and K_{zw} for DCF than those assumed may be appropriate for the high alcohol/acetone concentrations used to obtain the data in Fig. 8 [28], which would move the fitted curves to more negative potentials at pH <4. The low solubility of $DCFH_2$ or DCF at $pH < pK_{r1}$ or pK_{o2} impedes extension of studies to lower pH, which would have assisted in deriving pK_{s1}.

Analysis of the pH-dependent absorption spectrum of $DCFH_2$ suggested prototropic equilibria with $pK_{r2} \sim 7.9$ and $pK_{r3} \sim 9.2$ (cf. 2-chlorophenol, $pK_a \sim 8.6$). That both $DCFH_2$ and $DCFH^{\bullet}$ have pK_a values within 1 unit of typical physiological pH, as well as DCF being a weak acid with $pK_{o3} \sim 5.2$, has implications in comparing the results of experiments at different pH. Not only is the rate of peroxidase-like catalysis of $DCFH_2$ oxidation expected to vary significantly with pH over the region of most interest [35], the possible competition of oxygen with other electron acceptors for oxidation of $DCFH^{\bullet}$ to DCF could also be pH-dependent. Further, there is the potential for pH-dependent intracellular/extracellular and interorganelle concentration gradients of both $DCFH_2$ and DCF and the possibility of pH-dependent "leakage" or redistribution of both reduced probe and fluorescent product [36].

Although the use of quinone/semiquinone terminology is common in the present context, the value of the reduction potential $E°(DCF/DCF^{\bullet-}) = E°(o4/s4) \sim -0.86$ V is almost 1 V lower than that for 1,4-benzoquinone/semiquinone and around midway between the latter and that for typical ketyl radicals, e.g., $E°(Me_2CO/Me_2CO^{\bullet-}) = -2.1$ V [22]. The pK_a of the conjugate acid of 1,4-benzosemiquinone is ~4.1, compared to

pK_{s2} and pK_{s3} ~ 7–9 for DCFH$^{\bullet}$ and pK_a ~ 8.9 for the ketyl radical $H_2C{=}CHC^{\bullet}(OH)CH{=}CH_2$, which is a model for part of the structure of the tautomer s4′ in Fig. 1. These comparisons emphasize the existence of different resonance forms of the DCFH$^{\bullet}$ radical and point against too close identity of DCF as a typical quinone.

It is beyond the scope of this work to comment in any detail on the possible identity of alternative biological oxidants (other than oxygen) possibly reactive toward DCFH$^{\bullet}$. However, guidance may be derived from the value of the midpoint potential E_{mi}(DCF,H$^+$/DCFH$^{\bullet}$) ~ −0.75 V vs. NHE at pH$_i$ 7.4. This is much lower than the reduction potentials of most biological oxidants such as oxidized flavins, cytochromes, and other iron- or copper-containing metalloproteins. Such oxidants might therefore, in principle, become involved in probe chemistry at low oxygen tensions: note the high rate constants for oxidation of DCFH$^{\bullet}$/DCF$^{\bullet-}$ by $Fe(CN)_6^{3-}$ (~1.4×10^8 M^{-1} s^{-1} at pH 7.4). What is certain is that significant concentrations of redox-active agents such as menadione and 2,3-dimethoxy-1,4-naphthoquinone, commonly used to stimulate oxidate stress by redox cycling, have the potential to interfere with the use of $DCFH_2$ as an indicator, because with reduction potentials around −0.2 V they will clearly substitute competitively for oxygen as an efficient electron acceptor from DCFH$^{\bullet}$.

The measurements of reduction potential are also of relevance to the possibility that DCF, once formed, is reduced back to DCFH$^{\bullet}$ by cellular reductases such as NADPH:cytochrome *c* reductase. The value of $E_{m7.4}$(DCF,H$^+$/DCFH$^{\bullet}$) ~ −0.75 V measured in this work is considerably lower than the corresponding couple in many quinone substrates reactive toward common flavoprotein reductases [18], so this further complication now seems unlikely. However, the possibility that DCF can be reduced by more powerful reductants cannot be excluded. Of greatest relevance in the context of radical stress is the disulfide radical anion (RSSR$^{\bullet-}$), formed on conjugation of thiyl radicals (RS$^{\bullet}$) with thiol/thiolate (RSH/RS$^-$) [37]. Simple thiols have values of $E°$(RSSR/RSSR$^{\bullet-}$) around 0.8 V lower than E_{m7}(DCF,H$^+$/DCFH$^{\bullet}$) [38], and reduction of DCF by RSSR$^{\bullet-}$ is therefore likely to be a fast reaction. We have shown (unpublished work) that oxidation of $DCFH_2$ by RS$^{\bullet}$ is also fast and are currently working to characterize the kinetics of the various competing reactions, which are quite complex in the presence of oxygen, to help build a model of the possible involvement of thiol radical reactions in probe chemistry.

Conclusions

Despite reduced fluoresceins and similar probes having been used in around 2000 studies as an indicator of oxidative stress and related conditions in biological systems, and key properties identified which may restrict the usefulness of the probes, few basic chemical properties have been quantified. In this study, we have measured some of the prototropic equilibria that control the pH-dependent properties and have characterized the kinetics of the disproportionation reaction of the semiquinone radical to form the fluorescent product, the reactivity of the radical toward oxygen, and the reduction potential of the product, which helps define its susceptibility toward cellular reductases or other side reactions. The values of pK_a for the fully reduced probe and radical indicate that properties of both vary around physiological pH, with implications for pH-dependent concentration gradients and probe chemistry. The reduction potential of the fluorescent product is too low to suggest it is an effective substrate for cellular reductases, although reducing radicals derived from radical "scavenging" by thiols are likely to be reactive and thus present a further complication in the use of these probes.

Acknowledgments

This work was supported by Cancer Research UK. We thank Dr. Matthew Naylor for providing the tetraquat redox indicator and Dr. Edyta Madej for assistance with the cyclic voltammetry experiments.

References

[1] Keston, A. S.; Brandt, R. The fluorimetric analysis of ultramicro quantities of hydrogen peroxide. *Anal. Biochem.* **11:**1–5; 1965.

[2] Cathcart, R.; Schwiers, E.; Ames, B. N. Detection of picomole levels of hydroperoxides using a fluorescent dichlorofluorescein assay. *Anal. Biochem.* **134:**111–116; 1983.

[3] Rothe, G.; Valet, G. Flow cytometric analysis of respiratory burst activity in phagocytes with hydroethidine and 2′,7′-dichlorofluorescin. *J. Leukocyte Biol.* **47:**440–448; 1990.

[4] Royall, J. A.; Ischiropoulos, H. Evaluation of 2′,7′-dichlorofluorescin and dihydrorhodamine 123 as fluorescent probes for intracellular H_2O_2 in cultured endothelial cells. *Arch. Biochem. Biophys.* **302:**348–355; 1993.

[5] Rota, C.; Chignell, C. F.; Mason, R. P. Evidence for free radical formation during the oxidation of 2′-7′-dichlorofluorescin to the fluorescent dye 2′-7′-dichlorofluorescein by horseradish peroxidase: possible implications for oxidative stress measurements. *Free Radic. Biol. Med.* **27:**873–881; 1999.

[6] Burkitt, M. J.; Wardman, P. Cytochrome *c* is a potent catalyst of dichlorofluorescin oxidation: implications for the role of reactive oxygen species in apoptosis. *Biochem. Biophys. Res. Commun.* **282:**329–333; 2001.

[7] Ohashi, T.; Mizutani, A.; Murakami, A.; Kojo, S.; Ishii, T.; Taketani, S. Rapid oxidation of dichlorodihydrofluorescin with heme and hemoproteins: formation of the fluorescein is independent of the generation of reactive oxygen species. *FEBS Lett.* **511:**21–27; 2002.

[8] Lawrence, A.; Jones, C. M.; Wardman, P.; Burkitt, M. J. Evidence for the role of a peroxidase compound-I type intermediate in the oxidation of glutathione, NADH, ascorbate, and dichlorofluorescin by cytochrome *c*/H_2O_2: implications for oxidative stress during apoptosis. *J. Biol. Chem.* **278:**29410–29419; 2003.

[9] LeBel, C. P.; Ischiropoulos, H.; Bondy, S. C. Evaluation of the probe 2′,7′-dichlorofluorescin as an indicator of reactive oxygen species formation and oxidative stress. *Chem. Res. Toxicol.* **5:**227–231; 1992.

[10] Crow, J. P. Dichlorofluorescein and dihydrorhodamine 123 are sensitive indicators of peroxynitrite *in vitro:* implications for intracellular measurements of reactive nitrogen and oxygen species. *Nitric Oxide* **1:**145–157; 1997.

[11] Glebska, J.; Koppenol, W. H. Peroxynitrite-mediated oxidation of dichlorodihydrofluorescein and dihydrorhodamine. *Free Radic. Biol. Med.* **35:**676–682; 2003.

[12] Wrona, M.; Patel, K. B.; Wardman, P. Reactivity of 2′,7′-dichlorodihydrofluorescein and dihydrorhodamine 123 and their oxidized forms towards carbonate, nitrogen dioxide, and hydroxyl radicals. *Free Radic. Biol. Med.* **38:**262–270; 2005.

[13] Marchesi, E.; Rota, C.; Fann, Y. C.; Chignell, C. F.; Mason, R. P. Photoreduction of the fluorescent dye 2′-7′-dichlorofluorescein: a spin

trapping and direct electron spin resonance study with implications for oxidative stress measurements. *Free Radic. Biol. Med.* **26:**148–161; 1999.

[14] Bonini, M. G.; Rota, C.; Tomasi, A.; Mason, R. P. The oxidation of 2′,7′-dichlorofluorescin to reactive oxygen species: a self-fulfilling prophecy? *Free Radic. Biol. Med.* **40:**968–975; 2006.

[15] O'Malley, Y. Q.; Reszka, K. J.; Britigan, B. E. Direct oxidation of 2′,7′-dichlorodihydrofluorescein by pyocyanin and other redox-active compounds independent of reactive oxygen species production. *Free Radic. Biol. Med.* **36:**90–100; 2004.

[16] Rota, C.; Fann, Y. C.; Mason, R. P. Phenoxyl free radical formation during the oxidation of the fluorescent dye 2′,7′-dichlorofluorescein by horseradish peroxidase. *J. Biol. Chem.* **274:**28161–28168; 1999.

[17] Wardman, P.; Burkitt, M. J.; Patel, K. B.; Lawrence, A.; Jones, C. M.; Everett, S. A.; Vojnovic, B. Pitfalls in the use of common luminescent probes for oxidative and nitrosative stress. *J. Fluoresc.* **12:**65–68; 2002.

[18] Cenas, N.; Anusevicius, Z.; Bironaité, D.; Bachmanova, G. L.; Archakov, A. I.; Öllinger, K. The electron transfer reactions of NADPH:cytochrome P450 reductase with nonphysiological oxidants. *Arch. Biochem. Biophys.* **315:**400–406; 1994.

[19] Candeias, L. P.; Folkes, L. K.; Dennis, M. F.; Patel, K. B.; Everett, S. A.; Stratford, M. R. L.; Wardman, P. Free-radical intermediates and stable products in the oxidation of indole-3-acetic acid. *J. Phys. Chem.* **98:**10131–10137; 1994.

[20] Buxton, G. V.; Stuart, C. R. Re-evaluation of the thiocyanate dosimeter for pulse radiolysis. *J. Chem. Soc. Faraday Trans.* **91:**279–281; 1995.

[21] Ross, A. B.; Mallard, W. G.; Helman, W. P.; Buxton, G. V.; Huie, R. E.; Neta, P. NDRL-NIST solution kinetics database version 3. Notre Dame, IN, Notre Dame Radiation Laboratory and National Institute of Standards and Technology; 1998.

[22] Wardman, P. Reduction potentials of one-electron couples involving free radicals in aqueous solution. *J. Phys. Chem. Ref. Data* **18:**1637–1755; 1989.

[23] Wardman, P. The reduction potential of benzyl viologen: an important reference compound for oxidant/radical redox couples. *Free Radic. Res. Commun.* **14:**57–67; 1991.

[24] Albert, A.; Serjeant, E. P. The determination of ionization constants: a laboratory manual. Chapman & Hall, London; 1984.

[25] Clark, W. M. Oxidation–reduction potentials of organic systems. Williams & Wilkins, Baltimore; 1960.

[26] Bell, R. P. The proton in chemistry. Methuen, London; 1959.

[27] Capellos, C.; Bielski, B. H. J. Kinetic systems: mathematical description of chemical kinetics in solution. Wiley, New York; 1972.

[28] Mchedlov-Petrossyan, N. O.; Rubtsov, M. I.; Lukatskaya, L. L. Ionization and tautomerism of chloro-derivatives of fluorescein in water and aqueous acetone. *Dyes Pigments* **1992:**18; 1992.

[29] Leonhardt, H.; Gordon, L.; Livingston, R. Acid–base equilibria of fluorescein and 2′-7′-dichlorofluorescein in their ground and fluorescent states. *J. Phys. Chem.* **75:**245–249; 1971.

[30] Issa, I. M.; El-Samahy, A. A.; Issa, R. M.; Ghoneim, M. M. Polarography of dihalogen fluoresceins in solutions of varying pH at the DME. *Electrochim. Acta* **17:**1195–1202; 1972.

[31] Perlmutter-Hayman, B. The primary kinetic salt-effect in aqueous solution. *Prog. React. Kinet.* **6:**239–267; 1971.

[32] Lindqvist, L. A flash photolysis study of fluorescein. *Ark. Kemi* **16:**79–138; 1960.

[33] Cordier, P.; Grossweiner, L. I. Pulse radiolysis of aqueous fluorescein. *J. Phys. Chem.* **72:**2018–2026; 1968.

[34] Cadenas, E.; Davies, K. J. A. Mitochondrial free radical generation, oxidative stress, and aging. *Free Radic. Biol. Med.* **29:**222–230; 2000.

[35] Dunford, H. B. Heme peroxidases. Wiley-VCH, New York; 1999.

[36] Roos, A.; Boron, W. F. Intracellular pH. *Physiol. Rev.* **61:**296–434; 1981.

[37] Wardman, P.; von Sonntag, C. Kinetic factors that control the fate of thiyl radicals in cells. *Methods Enzymol.* **251:**31–45; 1995.

[38] Surdhar, P. S.; Armstrong, D. A. Reduction potentials and exchange reactions of thiyl radicals and disulfide anion radicals. *J. Phys. Chem.* **91:**6532–6537; 1987.